Theoretical analysis of the effect of doping and minority charge carrier life time in CIGS solar cells

H. A. MOHAMED*, Y. A. TAYA
Physics Department, Faculty of Science, Sohag University, 82524 Sohag, Egypt

In this work the optical and recombination losses for CuInGaSe (*CIGS*) thin-film solar cells have been theoretically studied. The optical losses have been studied on the basis of the thickness of frontal charge-collecting layer (*ZnO:Al*) effect. The recombination losses have been studied as a function of *CIGS* doping (N_A) and electron lifetime (τ_n). The optical and recombination losses effect on short circuit current density, (J_{sc}), the open circuit voltage (V_{oc}), the fill factor (*FF*) and conversion efficiency (η) of thin-film solar cells based on *n*-CdS/*p*-*CIGS* has been investigated. It was found that the film with the transparent conducting layer 100 nm thickness is suitable to give the highest J_{sc} value of about 29.5 mA/cm^2 and the lowest value of optical losses of about 26%. The *CIGS* doping has a significant effect on the values and behavior of the internal efficiency. There is a weak effect of the relaxation time on the efficiency of this solar cell as it increases from 18.7% to 19.1% with increase the lifetime from the value of 10 nS to 80 nS, respectively.

(Received July 20, 2020; accepted April 7, 2021)

Keywords: CIGS, Solar cell, Optical loss, Recombination loss and the efficiency

1. Introduction

Cu(In, Ga)Se_2 *(CIGS)* is considered one of the most promising second generation solar cells based on thin- film technologies with highest efficiencies which confirmed in the world. Tiwari group (EMPA Switzerland) reported recently a record efficiency of 20.4% on flexible polymer foil (23% in glass) [1]. The value 21.7% is the most recent record efficiency obtained in a laboratory environment [2-4]. There are large- area terrestrial applications of *CIGS* potential advantages, in addition *CIGS* photovoltaic can be made very lightweight and flexible which is desirable for building integrated and portable applications and have also shown high radiation resistance, compared to crystalline silicon and III-V cells so they are also promising for space applications [5, 6]. Many studied have concerned the optical, electrical and structural properties of each layer of thin-film solar cell such as the transparent conducting layer, n-type layer and the absorber layer [7-9]. Along with the experimental works, the solar cell modelling [10-15] has become indispensable tool used to analyse the performance and optimizing the design of any kind of efficient solar cells.

In this work, Mohamed model [16-19] have been used to study the effect of doping and electron lifetime on the *CIGS* solar cell performance. In this article the optical and recombination losses have been considered in *CIGS* devices, as it is important causes of low solar to electric energy conversion. The quantitative estimation of the optical losses has been carried out based on the optical constants of the used materials. On the other hand, the recombination losses at the front and the back surface of the absorber layer have been determined by using the continuity equation taking into account the drift and diffusion components of the photocurrent.

2. The simulation details

In this model, the absorber *CIGS* is a p- type, with different doping, the junction is made between the *CIGS* and n-type *CdS* which has a gap of 2.45 eV. The window layer is formed from *ZnO:Al* ceramic (ZnO 98 wt%, Al_2O_3 2 wt%) with a gap equals to 3.3 eV [20]. The data of CIGS were taken from Refs. [14, 21], where CIGS films were deposited by simultaneous thermal evaporation of elemental copper, indium, gallium and selenium. In this study, the spectrum was set to the global AM 1.5 standard and the operation temperature was maintained at 300 K. Through this model, the optical losses result from the reflection at air/*ZnO:Al, ZnO:Al/CdS, CdS/CIGS* interfaces and the light absorption in *ZnO:Al* and *CdS* layers as well as the recombination losses at the front and back surface of *CIGS* can be quantitatively assessment. The quantitative estimation of the optical losses is carried out passed on the refractive index, extinction coefficient and the optical band gap of the used materials. The recombination losses determined by employ the continuity equation that taking into account the drift and diffusion components of the photocurrent. The quantitative determination of the recombination losses is carried out based on the physical properties of the absorber layer (*CIGS*) such as; the absorption coefficient, energy band gap, thickness, carrier lifetime, mobility, etc. This study concerns on the effect of *CIGS* doping (N_A) and carrier life time (τ_n) on the solar cell efficiency.

2.1. CIGS solar cells structure

The schematic structure of substrate thin- film solar cell based on *CIGS* is shown in Fig. 1. The configuration of the *CIGS* layer can differ between different *CIGS* solar

cells, but they basically consist of front contact, a substrate, absorber, buffer layer and back contact. Soda lime glass is a common substrate. The soda lime glass used as a source of sodium that later is incorporated in the *CIGS* layer and increasing the conversion efficiency, allegedly by rare the defects at the *CIGS/CdS* junction or in the *CIGS* material [22, 23].

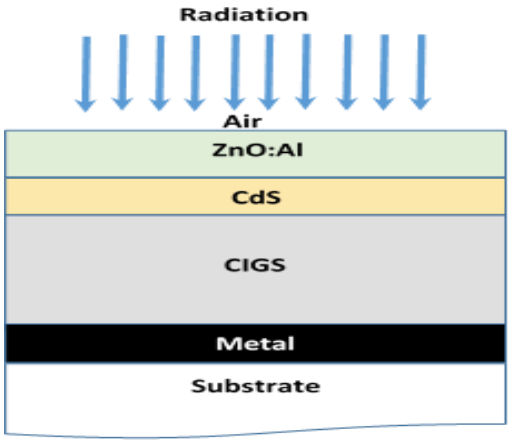

Fig. 1. Schematic cross-section of thin- film CIGS solar cell (color online)

A layer of molybdenum was sputtered onto the glass to form a back contact. Molybdenum is a good conductor and can allow sodium diffusion. A thick layer (2 μm) of *CIGS* is deposited on the molybdenum layer to act as the absorber. A thin (~ 60 nm) buffer layer of n- type *CdS* is usually deposited on the absorber to create a hetero junction. The required properties *of CdS* such as:, not too thick to reduce the absorption in the *CIGS* absorber layer, not too thin to avoid the short circuiting, relatively large conductivity to reduce the electrical solar cells losses, relatively high transparency and higher photoconductivity to not alter the solar cell spectral response [22]. The final layer is a *TCO* front contact; for example *ZnO:Al (AZO)* or In_2O_3:SnO_2 *(ITO).* This layer must be having some required properties such as: highly transparent (more than 85% in visible region), highly conducting at room temperature (sheet resistance less than 10 Ω/sq), and good adhesion to glass substrate [16]. The other parameters shown in Table 1.

Table 1. The parameters used in the model

parameter	φo-qV *(eV)*	N_D *(cm^{-3})*	ε	S_f (cm/s)	S_b (cm/s)	μ_n (cm^2/ V s)	μ_p (cm^2/ V s)
value	0.7	10^{15}	13.6	10^7	10^7	*20*	30

2.2. Reflection and absorption losses

The optical transmission $T(\lambda)$ that will reach the absorber layer, which is determined for *CIGS* cell by reflections from the interfaces air/ *ZnO:AL, ZnO:AL/CdS, CdS/CIGS* and absorption in the *ZnO:AL* and *CdS* layers needs to know in the calculations of short-circuit current density (J_{SC}) of solar cells. The reflectivity R at the interface between two contacting layers 1 and 2 can be determined based on the well- known Fresnel equation [16]:

$$R_{12} = \left(\frac{n_1 - n_2}{n_1 + n_2}\right)^2 \quad (1)$$

where n_1 and n_2 are the refractive indices of the two materials, respectively.

In the case of electrically conductive materials, the refractive index, $\bar{n}$ contains an imaginary part and is written as:

$$\bar{n} = n - ik \quad (2)$$

where n is the refractive index and k is the extinction coefficient. Therefore, the reflection coefficient R is written as:

$$R_{12}(\lambda) = \frac{|n_1^* - n_2^*|^2}{|n_1^* + n_2^*|^2} = \frac{(n_1 - n_2)^2 + (k_1 - k_2)^2}{(n_1 + n_2)^2 + (k_1 + k_2)^2} \quad (3)$$

The values of n and k of *ZnO:Al*, *CdS* and *CIGS* were taken from the literature data [24,25,14].

The transmittance can be determined using the optical calculation of the materials refractive indices and extinction coefficients. The transmission in this state is given by:

$$T(\lambda) = (1 - R_{12})(1 - R_{23})(1 - R_{34}) \quad (4)$$

where R_{12}, R_{23} and R_{34} are the reflectivity at the interfaces between air/*ZnO:AL*, *ZnO:AL/CdS* and *CdS/CIGS*, respectively.

The absorption process that takes place in *ZnO:Al* and *CdS* would considered in this part of the study. The losses due to reflection and absorption as mentioned previously, are called the optical losses. In this case, *Eq.(4)* takes the form:

$$T(\lambda) = (1 - R_{12})(1 - R_{23})(1 - R_{34})e^{-\alpha_1 d_1} e^{-\alpha_2 d_2} \quad (5)$$

where, α_1 and α_2 are the absorption coefficient of *ZnO:Al* and *CdS* and d_1 and d_2 their thickness, respectively.

The transmission of a transparent film of thickness d with refractive index n at normal incidence taking into account the interference is given by the Airy formula for multiple beam interference in a system of two parallel plane reflecting surfaces for the case of no absorption [26]

$$T(\lambda) = \frac{(1-R)^2}{(1-R)^2 + 4R\, sin^2(\frac{4\pi d}{\lambda})} \quad (6)$$

where R is the reflection coefficient of the film surface.

In Eq.(6), it is assumed that the film is in contact with identical materials at both sides. From our point of view, interference effects appear weaker if the film is in contact with materials having refractive index higher than that of air.

2.3. Recombination losses

The other important parameter that affects J_{SC} is the internal quantum yield (η_{int}). It is defined as the ratio between the photo generated electron– hole pairs and the total amount of the absorbed photons by the absorber layer. The optimal value of η_{int} =1. The variation of this unity is due to the recombination losses. The internal quantum efficiency of the solar cells is the summation of the drift and diffusion components, which are obliged to photogenerate of electron- hole pairs in the space- charge region and in the neutral part of the diode structure, respectively. The drift component of the internal quantum yield (η_{drift}) is given from the solution of the continuity equation in the form [27, 28]:

$$\eta_{drift} = \frac{1+\left(\frac{S_f}{D_p}\right)\left[\alpha+\frac{\left(\frac{2}{W}\right)(\varphi_o - qV)}{k_B T}\right]^{-1}}{1+\left(\frac{S_f}{D_p}\right)\left[\frac{\left(\frac{2}{W}\right)(\varphi_o - qV)}{k_B T}\right]^{-1}} - \exp(-\alpha W) \quad (7)$$

where, S_f is the recombination velocity at the front surface of *CIGS*, D_p is the diffusion coefficient of the holes related to the mobility μ_p by the Einstein relation $qD_p/ k_B T= \mu_p$, α is the absorption coefficient of *CIGS*, *W* is the width of space-charge region, *V* is the voltage, and φ_o is the barrier height. This equation takes into account the losses due to recombination at the *CdS/CIGS* interface, i.e., at the front surface of the absorber layer.

The diffusion component of the internal quantum efficiency (η_{dif}) is also given from the solution of the continuity equation [29]. The solution of the continuity equation was simplified with sufficient accuracy and can be written in the form [30],

$$\eta_{dif} = \frac{\alpha L_n}{\alpha^2 L_n^2 - 1} \exp(-\alpha W) \left\{ \alpha L_n - \frac{\left(\frac{S_b L_n}{D_n}\right)[\cosh((t-W)/L_n) - \exp(-\alpha(t-W))] + \sinh((t-W)/L_n) + \alpha L_n \exp(-\alpha(t-W))}{\left(\frac{S_b L_n}{D_n}\right) sinh\left[\frac{t-W}{L_n}\right] + cosh\left[\frac{t-W}{L_n}\right]} \right\} \quad (8)$$

where, α is the absorption coefficient of the absorber layer, D_n is the diffusion coefficient of the electrons related to the mobility μ_n by the Einstein relation $qD_n/k_B T= \mu_n$, ($L_n = \tau_n D_n$) is diffusion length of minority carriers, τ_n is the electron lifetime, *t* is the thickness of the absorber layer and S_b is the velocity of recombination at the back surface of *CIGS*. Equation (8) takes into consideration the recombination losses at the back surface of the absorber layer, i.e. at the *CIGS/MO* interface.

The total internal quantum yield (η_{int}) is easy to determine as the sum of all quantum yields.

$$\eta_{int} = \eta_{drift} + \eta_{dif} \quad (9)$$

The external quantum efficiency η_{ext} of the solar cells determined in the account of the optical losses owing to the reflection at different interfaces and absorption in *ZnO:Al* and *CdS*:

$$\eta_{ext} = T(\lambda)\, \eta_{int} \quad (10)$$

where $T(\lambda)$ is given by *Eq.(5)*, which takes into account the optical losses.

2.4. Short- circuit current density

The spectral distribution of the photons can be found as the spectral power (ϕ_i) versus the photon energy ($h\nu$). The short-circuit current density (J_{SC}) can be calculated according to this formula [31]:

$$J_{SC} = q \sum_i T(\lambda) \frac{\phi i\,(\lambda_i)}{h\nu_i} \eta_{int}(\lambda_i) \Delta\lambda_i \quad (11)$$

where $\Delta\lambda$ is the interval between neighbouring value of the wavelength, $T(\lambda)$ is given by *Eq. (5)* and $\eta_{int}(\lambda)$ is given by *Eq. (9)*.

According to the standard diode equation, the characteristic of *J*(V) for a single- junction solar cell under illumination can be written as the linear superposition of the dark characteristics of the cell and the photogenerated current:

$$J = J_0 \left[exp\left(\frac{qV}{AkT}\right) - 1 \right] - J_L \quad (12)$$

where J_0 is the reverse saturation current, J_L is the photogenerated current, q is the elementary charge, k is the Boltzmann constant, T is the absolute temperature and A is the ideality factor. The values of J_0 and A are taken from [32].

We can determine the losses (optical, recombination or both) using *Eq.(11)* and using the flowing expression:

$$Losses\ (\%) = \left(1 - \frac{Jsc}{J_{sc}^{max}}\right) \times 100 \qquad (13)$$

where J_{sc}^{max} is the maximum value of short- circuit current density, which can be obtained at $T(\lambda) = 1$ or $\eta_{int}(\lambda) = 1$. The summation in *Eq. (11)* should be made over the spectral range from $\lambda = 300$ nm to $\lambda = \lambda_g = hc/E_g$, where E_g is the optical band gap of the absorber layer.

The CIGS solar cell efficiency can be expressed by:

$$\eta = \frac{FF \times J_{SC} \times V_0}{P_{in}} \qquad (14)$$

where *FF* is the fill factor, V_{oc} is the open circuit voltage, P_{in} is the density of the total AM 1.5 solar radiation power.

The fill factor can be written as:

$$FF = \frac{J_m \times V_m}{J_{SC} \times V_0} \qquad (15)$$

2.5. Space charge width

The width of the space- charge region in the *CdS/CIGS* heterojunction can be expressed similarly to an asymmetric abrupt p-n junction [33]:

$$W = \frac{\varepsilon\, \varepsilon_0\, (\varphi_0 - qV)}{q^2\, (N_A - N_D)}^{\frac{1}{2}} \qquad (16)$$

where ε is the *CIGS* relative permittivity, ε_o is the electrical constant, $\varphi_0 = qV_{bi}$ is the barrier height at the *CIGS* side (V_{bi} is the built-in potential), q is the electron charge, V is the applied voltage, and N_A–N_D is the concentration of noncompensated donors in the *CdS* layer.

3. Results and discussion

Fig. 2 shows the transmission spectra of transparent conducting *ZnO:Al* layer and different thicknesses. The results are carried out using Eq.(6), which represents the interference effect. It is obvious that the interference increases with increasing the thickness of *ZnO:Al* from 50 nm to 200 nm. On other hand, the straight line in this figure represents the calculated transmission without interference (see Eq.(5)). It can be seen that there is no big difference in the average of the transmission between the two methods, however the using of interference equation is more accurate and realistic.

The short circuit current density (J_{sc}) of *CIGS* solar cell and the calculated optical losses shown in Fig. 3 with different values of *ZnO:Al* thicknesses. The highest value of J_{sc} of about 29.5 mA/cm^2 and the lowest value of optical losses of about 26% has been recorded for *CIGS* solar cell with *ZnO:Al* =100 nm. This indicates that the 100 nm thickness of the transparent conducting layer is suitable to obtain short- circuit current density of *CIGS* cells.

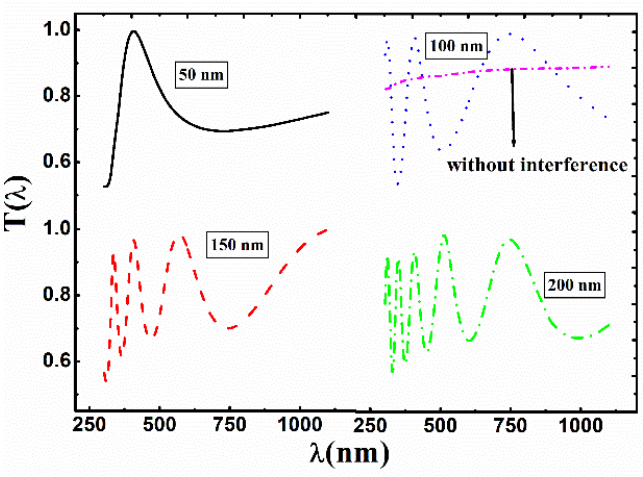

Fig. 2. The transmittance spectra of ZnO:Al layer with different thickness (50 – 200 nm) (color online)

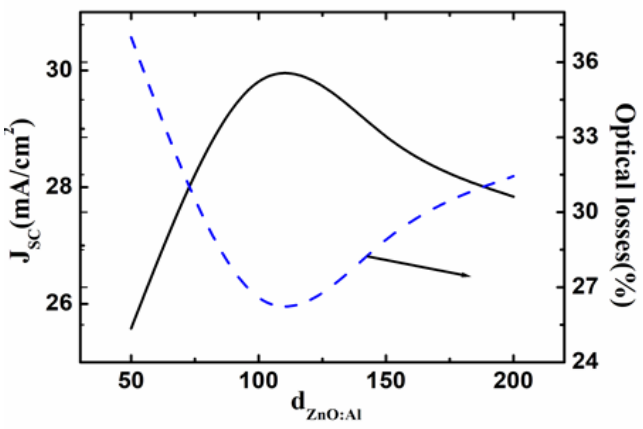

Fig. 3. The short circuit current (Jsc) and optical losses of CIGS solar cell with the different thickness of ZnO:Al layer (color online)

Both values of drift and diffusion component of internal quantum efficiencies have been calculated and plotted in Fig. 4. The results are achieved at different values of absorption coefficient (α) of *CIGS* layer and under the effect of different values of *CIGS* doping. It is obvious from Fig. 4 that the *CIGS* doping has a significant effect not only on the values of the internal efficiency but also on its behavior. Besides, the values of absorption coefficient have an obvious effect of drift component at high values of N_D (see Fig. 4-a), while the invers behavior of the diffusion component can be observed (see Fig. 4-b. From Fig. 4-c, we can note that the value of $\alpha = 1.5 \times 10^5$

cm^{-1} is sufficient to make *CIGS* absorbs most of the incident photons and there is no justification for increasing the absorption coefficient of the absorber layer to value greater than this. The quantum efficiency is seen to decrease with increasing the absorption coefficient. This result reflects that the electrons flux emitted towards the metal increase, which reduces the net photocurrent. As the bulk doping increase, this effect become smaller; because the strong doping lead to high electric field drives electrons away from the interface [34].

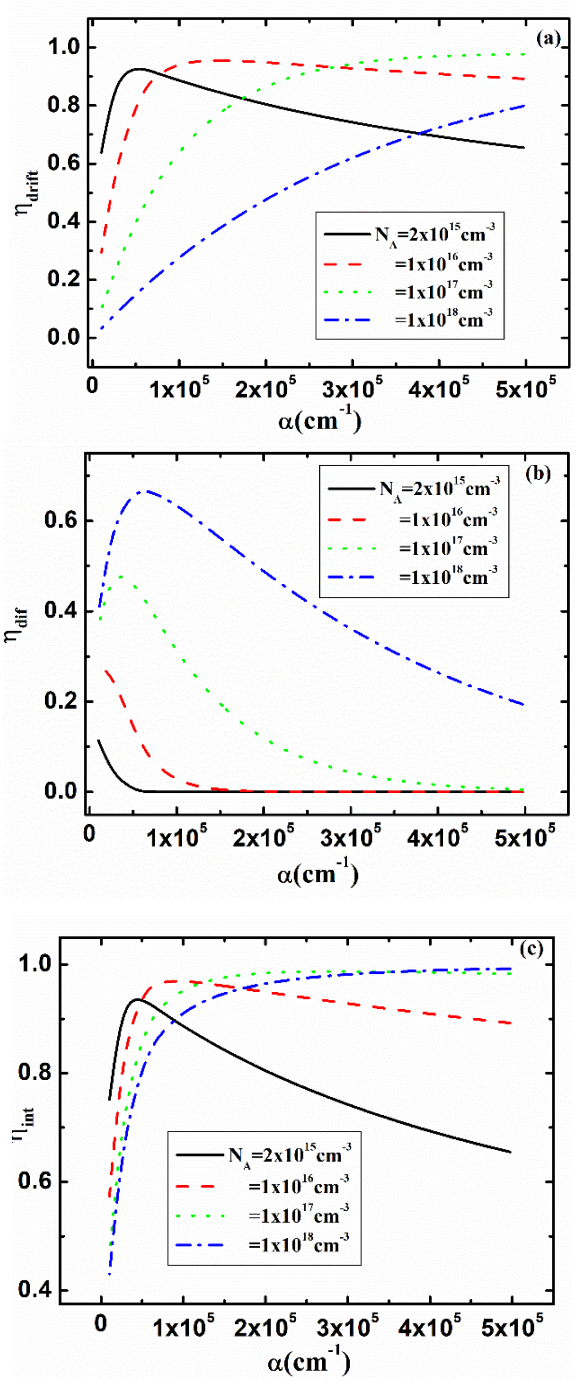

Fig. 4. (a) The drift component of internal quantum efficiency (η_{drift}), (b) The diffusion component of internal quantum efficiency (η_{dif}) and (c) The total internal quantum efficiency (η_{int}) of CIGS solar cell as a function of CIGS absorption coefficient (α) (color online)

With narrowing of the barrier region (increasing N_A or N_A-N_D), the internal quantum efficiency value decreases in the low-range of α because the larger portion of photons are absorbed outside of the space-charge region [28]. At long-range of α and for low N_A or N_A-N_D (also low electric field) the influence of surface recombination reveals itself where η records low values. With increasing N_A, the electric field increases and the effect of surface recombination becomes weaker. It can be noted that N_A = 10^{16}: 10^{17} cm^{-3} is suitable to give the highest value of the internal quantum efficiency.

Fig. 5a show the effect of N_A concentration on the drift, the diffusion and the short circuit current density. The diffusion current increases with increasing the N_A concentration but the drift current increases in the low concentration then decrease at higher concentration. This behaviors can be explained in the terms of Fig. 4.

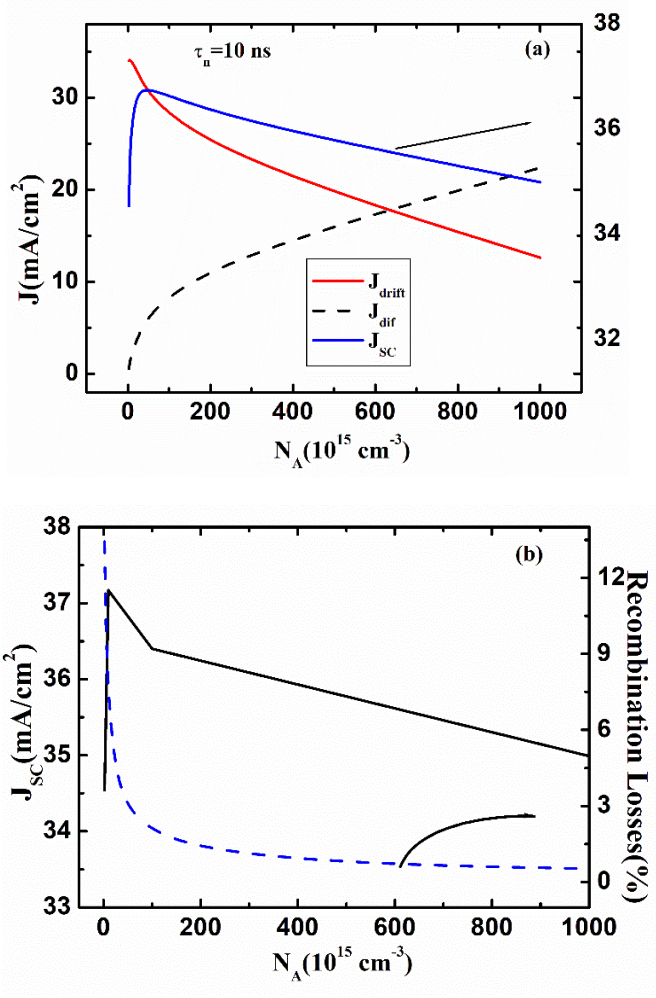

Fig. 5. (a) The current density of CIGS solar cell (with lifetime=10 nS) verses different values of CIGS doping and (b) The short circuit current density and recombination losses for CIGS solar cell with different values of doping concentration (color online)

In the low range of doping in (as shown in Fig. 5b), the short circuit current and the recombination losses have inverse behavior which is the logical result but at higher values of doping the short circuit current and the recombination losses decrease with doping increasing. This is due to at high N_A, the space-charge region width becomes smaller and it is not sufficient to absorb all the incident photons and hence J_{SC} decreases. However, the strong electric field which can take place in this case reduces the surface recombination. Most the values of recombination losses are in the range 1:3%.

Fig. 6 show the *J- V* curve for *CIGS* solar cell with different values of the lifetime from 10 ns to 80 ns. The results are carried out at $N_A = 10^{17}$ cm^{-3}. It can be seen that with increasing the lifetime of minority carriers (electrons), the curves slightly shifted downward. This indicate the weak effect of lifetime from 10 ns to 80 ns in the short circuit current density.

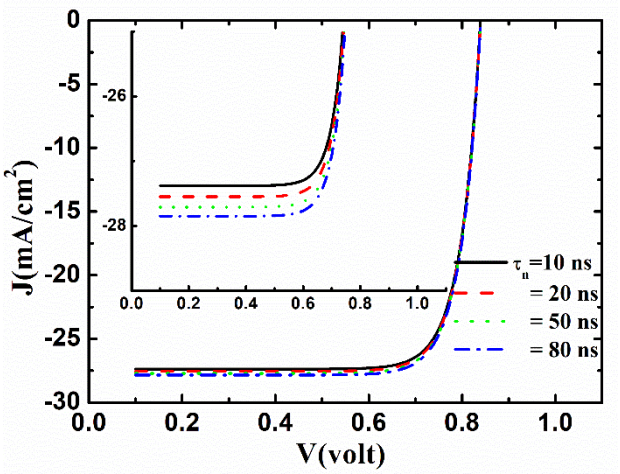

Fig. 6. (J- V) curve for CIGS solar cell with different values of the electron lifetimes (color online)

From Fig. 6, many factors such as the open circuit voltage (V_{OC}), fill factor (*FF*) and the cell efficiency (η) can be determined. The obtained results are plotted in Fig. 7 As can be shown in this figure, both the open circuit voltage and the efficiency of *CIGS* increase with increasing the lifetime from 10 ns to 80 ns. The efficiency reaches about 19.1% at lifetime of 80 ns. The fill factor initially decreases at small lifetime (10 ns to 30 ns) and then starts to slightly increase at long lifetime (from 30 ns to 80 ns).

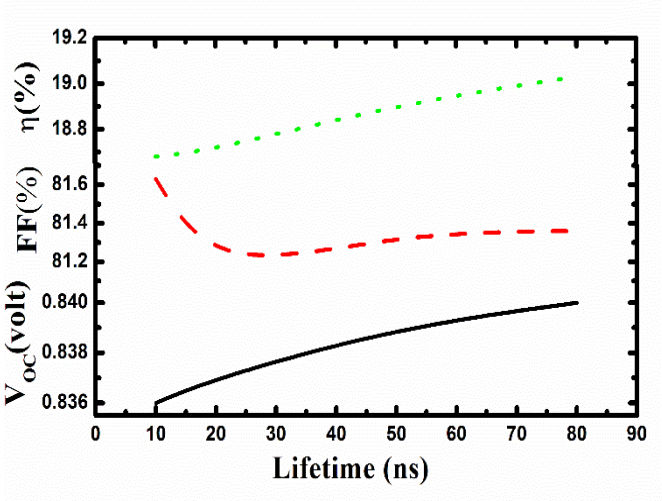

Fig. 7. The efficiency (η), Fill factor (FF) and open circuit voltage (V_{OC}) of CIGS solar cell with different electron lifetimes (color online)

4. Conclusion

Thin-film solar cell with structure *ZnO:Al/CdS/CIGS/Mo* has been studied as a function of the thickness of *ZnO:Al*, the absorption coefficient, the doping and electron lifetime of the absorber *CIGS*. The optical and surface recombination losses have been determined. The highest short-circuit current density has been recorded for *ZnO:Al* thickness equal to 100 nm. The absorption coefficient of 1.5×10^5 cm^{-1} and *CIGS* doping of 1×10^{17} cm^{-3} are the optimal values of the absorber layer. By increase the lifetime from 10 ns to 80 ns, there are weak change in the solar cell parameters as the open circuit voltage increase from 0.836 volt to 0.839 volt, the short circuit current from 27.5 to 27.8 mA/cm^2 and the efficiency increase from 18.7% to 19.1%.

References

[1] Jeyakumar Ramanujama, Douglas M. Bishopb, Teodor K. Todorovb, Oki Gunawanb, Jatin Rathc, Reza Nekoveid, Elisa Artegianie, Alessandro Romeoe, Progress in Materials Science **110**, 100619 (2020).

[2] P. Jackson, D. Hariskos, R. Wuerz, O. Kiowski, A. Bauer, T. M. Friedlmeier, M. Powalla, Phys. Status Solidi RRL, **9**(1), 28 (2015).

[3] M. A. Green, K. Emery, Y. Hishikawa, W. Warta, E. D. Dunlop, Solar cell efficiency tables (version 44), Prog. Photovolt **22**(7), 701 (2014).

[4] A. Belghachi, N. A. Limam, Chinese Journal of Physics **55**(4), 1127 (2017).

[5] F. Hasoon, Y. Yan, H. Althani, K. Jones, H. Moutinho, J. Alleman, M. Al-Jassim, R. Noufi, Thin Solid Films **387**(1-2), 1 (2001).

[6] M. G. Panthani, V. Akhavan, B. Goodfellow, J. P. Schmidtke, L. Dunn, A. Dodabalapur, P. F Barbara,

B. A. Korgel. Journal of Am. Chem. Soc. **130**(49), 16770 (2008).
[7] S. Antohe, L. Ion, V. A. Antohe, J. Optoelectron. Adv. M. **5**, 801 (2003).
[8] O. Toma, R. Pascu, M. Dinescu, C. Besleaga, T. L. Mitran, N. Scarisoreanu, S. Antohe, Chalcogenide Letters **8**, 541 (2011).
[9] L. Ion, I. Enculescu, S. Iftimie, V. Ghenescu, C. Tazlaoanu, C. Besleaga, T. L. Mitran, V. A. Antohe, M. M. Gugiu, S. Antohe, Chalcogenide Letters **7**(8), 521 (2010).
[10] S. Dabbabi, T. B. Nasr, N. K.Turki, Results in Physics **7**, 4020 (2017).
[11] S. Lee, K. Price, J. Park, Thin Solid Films **619**, 208 (2016).
[12] H. Heriche, Z. Rouabah, N. Bouariss, Int. J. Hydrogen Energ. **42**, 952 (2017).
[13] B. Vermang, W. J. Timo, V. Fjallstrom, F. Rostvall, M. Edoff, R. Kotipalli et al., Prog. Photovolt. Res. Appl. **22**(10), 1023 (2014).
[14] L. A. Kosyachenko, X. Mathew, P. D. Paulson, V. Ya. Lytvynenko, O. L. Aslyanchuk, Sol. Energy Mater. Sol. Cells **130**, 291 (2014).
[15] J. Liu, M. Zhang, X. Feng, Optik **172**, 1172 (2018).
[16] H. A. Mohamed, Journal of Applied Physics **113**(9), 093105 (2013).
[17] H. A. Mohamed, Thin Solid Films **589**, 72 (2015).
[18] H. A. Mohamed, Philosophical Magazin **94**(30), 3467 (2014).
[19] H. A. Mohamed, Solar Energy **108**, 360 (2014).
[20] Q. Xu, R. D. Hong, H. L. Huang, Z. F. Zhang, M. K. Zhang, X. P. Chen, Z. Y. Wu, Opt. Laser Technol. **45**, 513 (2013).
[21] P. D. Paulson, R. W. Birkmire, W. N. Shafarman, J. Appl. Phys. **94**, 879 (2003).
[22] J. H. Yoon, T. Y. Seong, J. Jeong, Prog. Photovolt. Res. Appl. **21**(1), 58 (2013).
[23] P. T. Erslev, J. W. Lee, W. N. Shafarman, J. D. Cohen, Thin Solid Films **517**(7), 2277 (2009).
[24] A. Y. Jaber, S. N. Alamri, M. S. Aida, Thin Solid Films **520**(9), 3485 (2012).
[25] S. Ninomiya, S. Adachi, Journal of Applied Physics **78**(2), 1183 (1995).
[26] L. A. Kosyachenko, E. V. Grushko, X. Mathew, Solar Energy Materials & Solar Cells **96**, 231 (2012).
[27] L. A. Kosyachenko, T. Toyama, Sol. Energy Mater. Sol. Cells **120**, 512 (2014).
[28] L. A. Kosyachenko, Semiconductors **40**, 710 (2006).
[29] S. M. Sze, K. K Ng, "Physics of Semiconductor Devices", 3rd, Wiley- Interscience, New Jersey, (2006).
[30] L. A. Kosyachenko, X. Mathew, P. D. Paulson, V. Y. Lytvynenko, O. L. Maslyanchuk, Sol. Energy Mater. Sol. Cells, **130**, 291 (2014).
[31] H. A. Mohamed, A. S. Mohamed, H. M. Ali, Mater. Res. Express **5**, 056411 (2018).
[32] W. Wang, M. T. Winkler, O. Gunawan, T. Gokmen, T. K. Todorov, Y. Zhu, D. B. Mitzi, Adv. Energy Mater. **4**(7), 1301465 (2014).
[33] L. A. Kosyachenko, X. Mathew, V. V. Motushchuk, V. M. Sklyarchuk, Solar Energy **80**(2), 148 (2006).
[34] M. Lavagna, J. P. Pique, Y. Marfaing, Solid-State Electronics **20**(3), 235 (1977).

*Corresponding author: hussein_abdelhafez2000@yahoo.com